Performance of Blind Deconvolution and Super Resolution Image Reconstruction

Seiichi Gohshi and Michikazu Akasu
Kogakuin University, 1-24-2, Nishi-Shinjuku, Shinjuku-Ku, Tokyo, Japan

Keywords: Super Resolution, Super Resolution Image Reconstruction, Low Resolution Image, High Resolution Image, Blur.

Abstract: Super Resolution (SR) is a technique for improving the resolution of digital images. Super Resolution Image Reconstruction (SRR) is one of the most common SR techniques. However, in addition to SRR, there are several other techniques to improve image resolution. A technique called Blind Deconvolution (BD) has been used to process out of focus images in the field of astronomy. When BD was first described, in the 1970s, it was not considered to be a viable candidate to be used for SR. However, the process of improving resolution is very similar to that of focusing images. SRR and BD both use iterations to create a high quality image from low resolution images. Compared with SRR, BD comes with some disadvantages. For example, algorithms sometimes cause divergences or limit cycles which means that the high resolution image cannot be obtained. In this study, we describe a method of fixing the issues that prevent BD from achieving a high-resolution image using simulation to increase its stability. The output from the improved algorithm for BD is compared with the current SR technique, SRR. We show that the BD technique is in fact superior to SRR.

1 INTRODUCTION

As image and video systems have developed, the focus has always been on improving the quality of the image. Resolution is one of the important factors in the quality of images and videos; therefore, considerable research effort has gone into improving resolution. As a result, the resolution of images has dramatically improved since the turn of the century. High-resolution cameras capture high-resolution images and videos using CMOS imaging sensors. Cameras using such sensors are built into smartphones and the security cameras that monitor city life. High-resolution displays are available at affordable prices; therefore, many individuals can view and manipulate images and videos. However, the resolution of images and videos may not be adequate to match the sensitivity of the displays used to view them. For example, we might view an image with resolution suitable for HDTV [(2K) 1,920 1080 pixels] on a screen with a higher resolution, such as 4K (3,840 2,160 pixels)]; the image should be converted from 2K to 4K. Currently, even smartphones are equipped with 4K displays and 8K displays will be available on the market in the near future. Enlargement blur always results from a mismatch between image resolution and display sensitivity. Enlargement blur also occurs in several other cases. For example, when part of the image from a security camera image is enlarged to take a close look at the person of interest or when analog TV content is converted to the 2K format. Enhancement is a technique often used to improve image quality (Schreiber, 1970) (Pratt, 2001) particularly in commercial products. However, it has its drawbacks. The enhancement process only amplifies the edges in the image. It cannot create thinner edges from higher frequency elements that the input image did not have.

Super Resolution (SR) is another approach with similar objectives. SR research started in the late 1990s (Patti et al., 1997)(Elad and Feuer, 1997). Super resolution image reconstruction (SRR) is one of the most popular approaches and has generated many papers (Patti and Altunbasak, 2001)(Park et al., 2003)(Farsiu et al., 2004)(Panda et al., 2011)(van Eekeren et al., 2010)(Sanchez-Beato and Pajares, 2008)(Protter et al., 2009)(Katsaggelos et al., 2007)(Chaudhuri, 2001)(Chaudhuri and Manjunath, 2005)(Bannore, 2009)(Devi et al., 2014). SRR is a technique that uses low resolution images (LRIs) to create a high-resolution image (HRI) using iterations.

Historically, this image restoration approach has dominated the field of SR. They are both focused

Gohshi, S. and Akasu, M.
Performance of Blind Deconvolution and Super Resolution Image Reconstruction.
DOI: 10.5220/0006467400690076
In *Proceedings of the 14th International Joint Conference on e-Business and Telecommunications (ICETE 2017) - Volume 5: SIGMAP*, pages 69-76
ISBN: 978-989-758-260-8

on improving the quality of the image (Andrews and Hunt, 1997)(Banha and Katsaggelos, 1997). Wiener filtering is also widely used (Petrou and Edition, 2011). Wiener filtering works mainly by restoring an image degraded by noise. However, the performance of the algorithm is not very good. Blind deconvolution (BD) is another approach for restoring an out of focus image. It has been mostly used in astronomy (Richardson, 1972a)(Lucy, 1974). Image restoration techniques are categorized in image restoration field. However, BD works for blurry images and improves resolution. Recently, BD has been categorized as SR (Harmeling et al., 2009)(Harmeling et al., 2010)(Begin and Ferrie, 2004)(Sroubek et al., 2007); however, these researchers did not show that BD performed better in enlarging blurred images compared with the typical SR technique, SRR. In their BD studies, the size of the output image is the same as that of the input image. SRR techniques, in contrast, are used for image enlargement wherein the input images are smaller than the output images. In practical SR applications, we cannot always use multi-frames. However, SRR uses multi-LRIs, whereas BD uses only one image.

In this study, we discuss the performance of BD for the enlargement of blurred images and compare its performance with that of the most widely used SR technique, SRR. BD has the following drawbacks: it sometimes causes diverges or limit cycles to a different image and cannot obtain HRI with the iterations. In this study, an idea to fix these issues is proposed. This paper is organized as follows. In Section 2, the algorithm of SRR is explained. In Section 3, we present the meaning of SR and the dene the term of LRI as used in SR. In Section 4, the new BD algorithm is explained. In Section 5, experimental results obtained using BD and SRR are compared. Section 6 is the conclusion of the paper.

2 SRR

SRR does not suffer from the issues of BD discussed in the previous section. SRR rarely causes divergences, or limit cycles to a different image. However, SRR has a serious limitation: it can work only when LRIs are aliasing. In this section, we discuss the limitations of SRR that are distinct from those of BD. Figure 1 shows the basic idea of SRR (Farsiu et al., 2004). The first step is to process the HRI with a low pass filter (LPF). The cut-off frequency of the LPF is higher than the Nyquist frequency of the LRIs. LRIs are created from HRI with sub-sampling and all LRIs have aliasing. All LRIs are distinct since the sampled pixel phases of each LRI are different. The summation of sampled pixels exceeds the pixels in the HRI. For example, suppose we want to make 256 256 pixel LRIs from a 512 512 pixel HRI. In this case, four LRIs would have the same pixels as the HRI; however, SRR must create more than four 256 256 images to reconstruct HRI. That is, we need a larger amount of information than is in the HRI in order to reconstruct it with SRR. The LRIs are thus composed by iteration, minimizing the cost function to recreate the HRI.

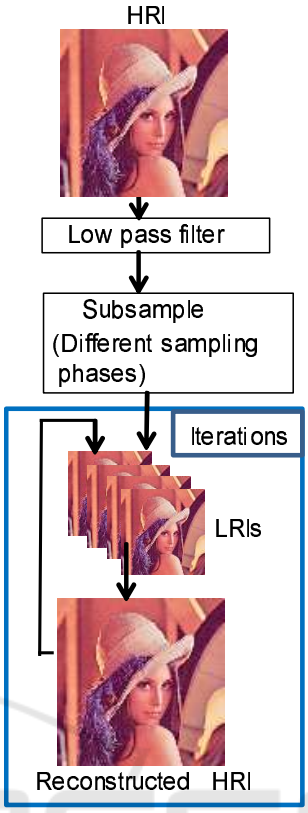

Figure 1: SRR algorithm.

There have been several SRR proposals for the cost function (Farsiu et al., 2004)(Park et al., 2003)(Panda et al., 2011)(van Eekeren et al., 2010). They all have a similar aim to minimize the cost function, which comprises the sum of L_n. In particular, L_1 and L_2 are commonly used. L_n is called the Norm and $n = 1, 2, \cdots$. Minimizing the cost function (1) was proposed by (Farsiu et al., 2004) , that of (2) was proposed by (Panda et al., 2011) and that of (3) is proposed by (van Eekeren et al., 2010).

$$\underline{\hat{X}} = ||\underline{Y} - H\underline{X}||_2^2 + \lambda\gamma(\underline{X}) \quad (1)$$

$$J(X) = ||Y - HY||^2 + \lambda||X||^2 \quad (2)$$

$$C_{p,f} = \frac{1}{KM\delta_n^2}\sum_{k=1}^{K}\sum_{m=1}^{M}(y_{k,m}-\widetilde{y}_{k,m}(\mathbf{p},\mathbf{b},\mathbf{f}))^2 \quad (3)$$
$$+\frac{\lambda_f}{Q}\sum_{h,v=0,1}^{h+v=1}||\mathbf{f}-S_x^h S_y^v\mathbf{f}||_H$$
$$\lambda_p(\frac{||\mathbf{P}||}{P})\sum_{p=1}^{P}\Gamma_P(\mathbf{P})$$

It is not, however considered to be possible to define just one cost function for all the various images. Although one cost function may produce a good result for one image, it may give a poor result for another image for which a different cost function gives a better result (Farsiu et al., 2004).

However, it is not possible to dene one cost function for all the various images. Although one cost function may produce a good result for one image, it may give a poor result for another image (Farsiu et al., 2004). The iterations are essential for SRR to reconstruct HRI from LRIs. The result of iterations must converge to the HRI. However, the result may diverge if the cost function or some other functions such as sampling phases are not appropriate. The number of iterations is also an issue. The time consumed by the iterations is in proportion to their number. A small number is required for practical applications. Much research has already gone into finding solutions to these problems, which are called Fast and Robust. In our opinion, much more important issues such as the ultimate highest resolution produced with SRR need to be addressed. If the convergence point of SRR is just the HRI, as shown in Figure 1, SRR would not improve the resolution of the original HRI at all.

The algorithm in Figure 1 shows that the role of the LPF is very important. Without the LPF Figure 1, the process is just breaking down the HRI into LRIs and reconstructing the HRI with LRIs. It is just making a jigsaw puzzle with the LRIs and then solving it again by minimizing the complex cost function. The result resolution of SRR depends on the characteristics of the LPF and it is necessary for LRIs to contain aliasing (Farsiu et al., 2004)(Glasner et al., 2009).

Figure 2: Example of LRI (taken from (Farsiu et al., 2004)).

The typical LRIs for SRR for a video are shown in Figures 2 and 3 (Farsiu et al., 2004)(van Eekeren et al., 2010). Images in Figures 2 and 3 are taken

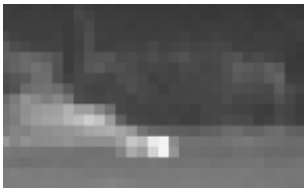

Figure 3: Example of LRI (taken from (van Eekeren et al., 2010)).

Figure 4: Moving object (Digital still camera).

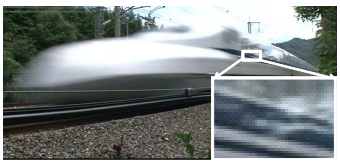

Figure 5: Moving object (Video camera).

with an infrared camera. Infrared cameras have very high sensitivity compared with general HDTV video cameras and SDTV video cameras. Although these images were taken by video cameras, there is not motion blur. It has not been mentioned that SRR cannot work images that has motion blur. This is one of the limitations of SRR. Digital still cameras can take photographs at high shutter speeds. Some professional video cameras shutters can reduce motion blur. However, we rarely can use a shutter even if the video camera has it because the photoelectric sensors of video cameras do not have high sensitivities. If we use the shutter in a professional video camera, the resulting images may be very noisy Figures 4 and 5 are photographs taken of the same object with a digital still camera and a video camera and are displayed at HDTV resolution. Since we are discussing SRR for videos, cameras and displays must be compatible with HDTV resolution as a general standard for video systems. There are other special cameras such as high speed cameras and infrared cameras and special displays such as Super HDTV (SHV) displays and high dynamic range displays. However, they do not fall into the general category. While Figure 4 has details and aliasing around the moving object, Figure 5 does not have any. The difference between them was caused by the shutter.

It is necessary for LRIs for SRR to have aliasing. The block shapes in Figure 2 and Figure 3 are caused by aliasing. In particular, when the image in Figure 3 was taken, the camera was gently shaken to provide

sub-pixel motion within the field of view of the camera (van Eekeren et al., 2010). This condition would not occur in practical applications such as movie content and TV content.

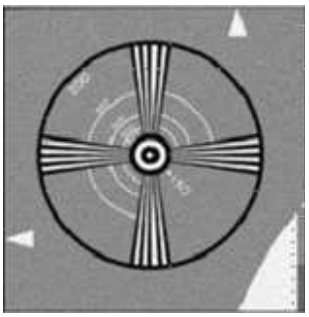

Figure 6: HRI.

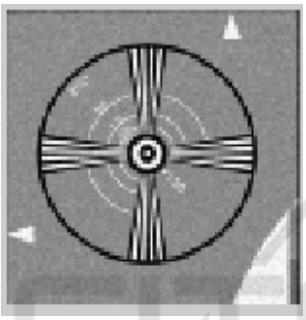

Figure 7: LRI for SRR.

Figure 8: Blurry image.

3 MEANING OF SR

Here we have to think about the meaning of SR. Whenever the term SR is used, it signifies a way of improving resolution. In an earlier SR research, the original image was the HRI shown in Figure 6. LRIs were made using the algorithm shown in Figure 1. HRI was processed with a low pass filter and subsampled to create LRIs. Figure 7 shows an LRI characteristic of those discussed in SRR papers. It is over-sharpened with aliasing due to high frequency elements. According to the Nyquist theorem, a pre-filter is necessary to reduce the bandwidth not to cause aliasing. In most cases, as far as the SR research goes, LRIs are created under the conditions that do not meet the requirements of the Nyquist sampling theorem. It means making LRIs with aliasing and then reconstructing the HRI from those LRIs by reducing aliasing. If the LRIs were created under the conditions of the Nyquist sampling theorem, they would not have the aliasing shown in Figure 8. If Figure 8 was used as the LRI, SRR would not be able to reconstruct the HRI.

We have to think about the meaning of SR and LRI. For the practical application of the SR technique, the image needs to be enlarged and the details of the image need to be enhanced. Enlarging an image always causes enlargement blur. It does not create the image shown in Figure 7 but the image shown in Figure 8. Figure 8 should be used as the input LRI for SR to process and improve its resolution. Moreover, many LRIs are not suitable for practical applications. In general, we can use only one LRI. The conclusion of this Section is that SR would improve resolution from only one of the blurred images: the one shown in Figure 8.

4 BLIND DECONVOLUTION (BD)

4.1 BD Algorithm

When we capture an image of an object, we capture the beams of light that are reflected on the surface of the object. After being reflected, the beams are diffracted, diffused, and/or reflected in the space and lens of the camera until they reach the imaging device in the camera. These factors degrade resolution and make the images blurry. Here we define $\psi(x,y)$ as the true image and $\phi(x,y)$ as the observed blurry image. (x,y) denotes the two dimensional vector. The relationship between $\psi(x,y)$ and $\phi(x,y)$ (Richardson, 1972a)(Lucy, 1974) can be presented as follows.

$$\phi(x,y) = \int\int \psi(\xi,\eta)P(x-\xi,y-\eta)d\xi d\eta \qquad (4)$$

Here, ξ and η are introduced to calculate the horizontal and vertical convolution.

$$\psi(x,y) = \int\int \phi(\xi,\eta)Q(x-\xi,y-\eta)d\xi d\eta \qquad (5)$$

Here, $P(\cdot,\cdot)$ is the blur factor and $Q(\cdot,\cdot)$ is the inverse filter of $P(\cdot,\cdot)$ (Richardson, 1972a). $P(\cdot,\cdot)$ is called the point spread function (PSF) and generally it has a Gaussian shape characteristic (Richardson, 1972a). These are filtering processes between $\phi(x,y)$and $p(x,y)$.

The blurry image can be restored by finding $P(x,y)$. Since this is a typical inverse problem, it is impossible to solve it using a direct method (Petrou and Edition, 2011). Instead, of a direct method, an iterative method is proposed. Lucy, 1974 showed that $\phi(x,y)$ can be obtained as follows. Using the Bayesian inference, we obtain the following equation.

$$Q^r(x-\xi,y-\eta) = \frac{P^r(x-\xi,y-\eta)\psi^r(x,y)}{\phi^r(x,y)} \quad (6)$$

Here r is the iteration number. In Equation (5), $\phi(\xi,\eta)$ is the original blurry image and we define it as $\phi^0(\xi,\eta)$ as the initial image.

Plugging Equation (6) into Equation (5), we obtain the following formula.

$$\begin{aligned}\psi^{r+1}(x,y) &= \int\int \psi^r(x,y)\frac{\phi^0(x,y)}{\phi^r(x,y)}P^r(x-\xi,y-\eta)d\xi d\eta \\ &= \psi^r(x,y)\int\int \frac{\phi^0(x,y)}{\phi^r(x,y)}P^r(x-\xi,y-\eta)d\xi d\eta\end{aligned} \quad (7)$$

Here, we transform Equation (4) with the iteration number r.

$$\phi^r(x,y) = \int\int \psi^r(x-\xi,y-\eta)P^r(\xi,\eta)d\xi d\eta \quad (8)$$

Using Equation (6), we also obtain the recursion equation of r about PSF,

$$\begin{aligned}&P^{r+1}(x,y) \\ &= P^r(x,y)\int\int \frac{\phi^0(x,y)}{\phi^r(x,y)}\psi^r(x-\xi,y-\eta)d\xi d\eta\end{aligned} \quad (9)$$

We define a scalar value $E(r)$ to evaluate the convergence.

$$E(r) = \int\int |\phi^r(x,y) - \phi^{r-1}(x,y)|dxdy \quad (10)$$

Equation 10 is called L1 norm. Equation 10 is an indicator of the iterations process. It decreases during the convergence process.

Using the recursion Equations (7), (8), (9), Equation 10 and the iterations, we can obtain $\psi(x,y)$, HRI and $P(x,y)$, PSF. The algorithm is called the Lucy (Lucy, 1974) and Richardson (Richardson, 1972b) algorithm and it is used in astronomy to refocus images of planets star constellations.

4.2 Problems of BD

BD is a method for calculating the true image and PSF together with iterations. During the iterations, the blurry image and PSF gradually converge to the true image and the true PSF. However, the iterations sometimes causes divergences or fall down to the limit cycles. In these cases, the BD cannot create the true image and PSF. Figure 9 is the original image. Figure 10 shows a blurry image that is created from Figure 9 processed with a Gaussian low pass filter ($\sigma = 3.0$, kernel 15×15). If we use BD for Figure 10, BD causes divergence that creates Figure 11 as the result image and Figure 12 as PSF. In the BD process the shape of PSF is very important. Figure 13 shows a typical shape of PSF. However, the PSF shape of Figure 12 spreads in diagonal directions that emphasize oblique frequency elements. The oblique frequency elements amplify oblique edges and create the diagonal ringing shown in Figure 11. It is a kind of divergence.

Figure 9: Original image.

Figure 10: Gaussian filter ($\sigma = 3.0$ kernel 15×15)processed.

Figure 11: Example of divergent image.

4.3 Proposed Method

In general, our interests tend to focus on the quality of the resulting image. However, in the BD process, image degradation is caused by the irregular shape of

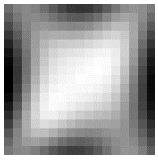

Figure 12: Example of divergent PSF.

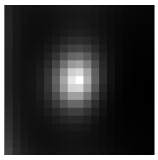

Figure 13: Example of PSF.

PSD. We investigated the change of the PSD shape during the iterations and made an interesting observation. In the BD iteration process of the previous section, Figure 10, the PSF became Figure 14. Although in general, PSD has symmetrical Gaussian shape, Figure 14 is asymmetrical. The asymmetrical PSF generates a divergent image during the iterations. When the $E(r)$ value of Equation 10 increases, we rotate the PSF form 180^0, arriving at Figure 15, and then continue the iterations. This process produced the PSF shown in Figure 16 and the resulting image is shown in Figure 17. Compared with Figure 10, Figure 17 has been restored and it has higher resolution. According to the experiments, the rotation introduced into the PSF method works when the iterations causes divergence. According to our simulations, it also decreases limit cycles.

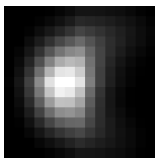

Figure 14: Asymmetry PSF.

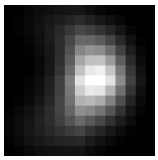

Figure 15: Rotation PSF of Figure 14.

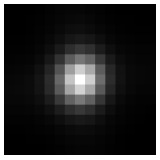

Figure 16: Convergence PSF of Figure 14.

Figure 17: BD processed image for 10.

5 EXPERIMENT

Since SRR is one of the most common SR techniques, we compare the performance of BD with that of SRR. The algorithm of SRR that creates HR from LRIs is explained in Section 2 and Figure 1. Instead of SRR, we use BD to improve the resolution of an image, as shown in Figure 18. HRI is processed with a low pass filter (LPF) to limit the bandwidth and subsample to create a LRI. LRI is enlarged with a digital filter and a blurry image is obtained. The blurry image is processed with BD and HRI is created. Both SRR and BD can create HRI from LRIs/LRI. Two points should, however, be noted. First, SRR needs multiple LRIs, whereas BD needs only one LRI. Second, the characteristics of LPFs are different. In SRR (Figure 1), the bandwidth of the LPF is wide and aliasing occurs when LRIs are created. In contrast, in the LPF in Figure 18, the LRI created by the subsample does not have aliasing. Therefore, the bandwidth of LPF is narrow enough to satisfy the Nyquist sampling theorem. In SR, the quality of the reconstructed HRI is the most important. Many SRR papers evaluated qualitatively the outputs from their applications of SRR, i.e., the comparison between the original HRI and the reconstructed HRI in Figure 18. Here we evaluate SRR and BD quantitatively with the peak signal to noise ratio (PSNR). Although there are many SRR papers, most of them include only a qualitative comparison. We chose four papers that show the PSNR values (Youmin et al., 2016) (Yin et al., 2016) (Shah et al., 2013) (Jahanbin and Naething, 2005). Their subsample ratios are 2:1, i.e., the same as the algorithm shown in Figure 18. We conducted computer simulations of the proposed BD algorithm. The images used are the famous ones of Lena and Mandrill. In our simulations, the resolution of HRI is 512×512 and that of LRI is 256×256, which means the subsample ratio is 2:1. Table 1 shows the comparison results between the proposed BD method and SRR. In two papers (Youmin et al., 2016) (Shah et al., 2013),

Mandrill was not used. Table 1 shows that the performance of BD as the SR capability outperforms SRR.

Initially, BD was proposed for astrophotography to improve the out-of-focus images. However, we have shown in this paper that BD can be used for SR and outperform the most common SR techniques. Due to space limitations, the comparison between learning-based SR and BD cannot be discussed here. This is the next step in this research.

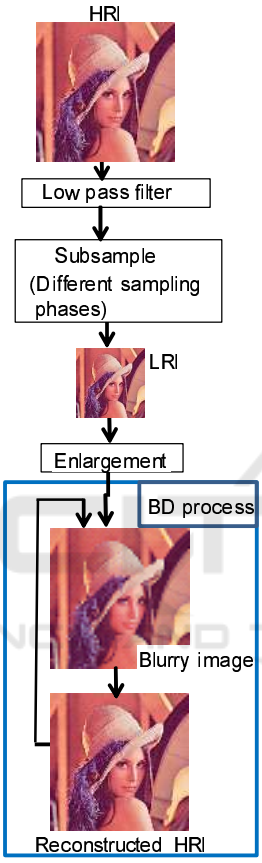

Figure 18: BD algorithm.

Table 1: Quantitative Performance Comparison Using PSNR.

	Lena	Mandrill
(Youmin et al., 2016)	29.2142	-
(Yin et al., 2016)	23.4060	22.2895
(Shah et al., 2013)	23.3731	-
(Jahanbin and Naething, 2005)	23.509	19.461
Proposed method	35.041d	24.164

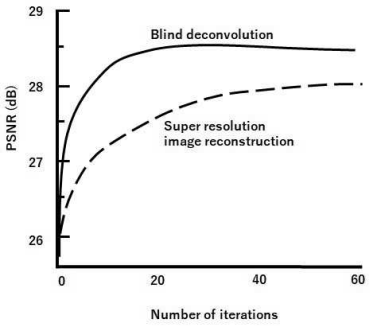

Figure 19: Convergence speed of BD and SRR.

6 SPEED OF CONVERGENCE

BD and SRR need iterations to converse on the HRIs. Figure 19 shows the relations of the BD and SRR. The horizontal axis is the iteration number and the vertical axis is the peak signal to noise ratio (PSNR). The two curves show the changes of PSNR to the iterations. As the iteration progresses the PSNR values improve. However, the behaviors of the PSNR values of BD and SRR are different. The PSNR value of BD is better than that of SRR and it is almost saturated at the 20 times iterations. It means that BD converges on HRI faster than SRR. Iterations are heavy load for SR technologies. If the numbers of the iterations become smaller, it means the decreasing of the calculations costs. According to the simulation result, BD is superior to SRR about the cost.

7 CONCLUSION

The capability of BD is discussed. BD was proposed to refocus astrophotographs. This is a similar idea to SR, which creates HRI from LRIs. However, BD comes with some issues, such as falling in divergences or limit cycles. In this study, a method to fix these issues was proposed. Using this method, BD capability was compared with the typical SR technique, SRR. According to the simulation results, BD outperformed SRR about the image quality and cost. Comparing BD with another common SR, learning-based SR is the next step.

REFERENCES

Andrews, H. and Hunt, B. (1997). *Digital Image Restoration.* Englewood Cliffs, N.J. : Prentice-Hall.

Banha, M. and Katsaggelos, A. (1997). Digital image restoration.

IEEE Signal Processing Magazine, 14(2):24–41.

Bannore, V. (2009). *Iterative-Interpolation Super-Resolution Reconstruction*. Springer.

Begin, I. and Ferrie, F. R. (2004). Blind super-resolution using a learning-based approach. *ICPR 2004*, 2:85–89.

Chaudhuri, S. (2001). *Super-Resolution Imaging*. Kuliwer Academic Publishers.

Chaudhuri, S. and Manjunath, J. (2005). *Motion-Free Super-Resolution*. Springer.

Devi, A. G., Madhu, T., and Kishore, K. L. (2014). An improved super resolution image reconstruction using svd based fusion and blind deconvolution techniques. *International Journal of Signal Processing, Image Processing and Pattern Recognition*.

Elad, M. and Feuer, A. (1997). Restoration of a single superresolution image@from several blurred, noisy, and undersampled measured images. *IEEE Trans. Image Processing*, 6(12):1646–1658.

Farsiu, S., Robinson, D., Elad, M., and Milanfar, P. (2004). Fast and robust multi-frame super-resolution. *IEEE Transactions on Image Processing*.

Glasner, D., Bagon, S., and Irani, M. (2009). Super-resolution from a single image. *International Conference on Computer Vision (ICCV)*.

Harmeling, S., M. Hirsch, S. S., and Scholkopf, B. (2009). Online blind image deconvolution for astronomy. *IEEE Conference on Comp. Photogr.*

Harmeling, S., Sra, S., Hirsch, M., and Scholkopf, B. (2010). Multiframe blind deconvolution, super-resolution, and saturation correction via incremental em. *Proceedings of 2010 IEEE 17th International Conference on Image Processing*, pages 3313–3316.

Jahanbin, S. and Naething, R. (2005). Super-resolution image reconstruction performance.

Katsaggelos, A., Molona, R., and Mateos, J. (2007). *Super Resolution of Images and Video, Synthesis Lectures on Images, Video and Multimedia Processing*. Morgan & Clayppo Publishers.

Lucy, L. B. (1974). An iterative technique for the rectification of observed distributions. *The Astronomical Journal*, 79(6):745–754.

Panda, S., Prasad, R., and Jena, G. (2011). Pocs based super-resolution image reconstruction using an adaptive regularization parameter. *IEEE Transactions on Image Processing*.

Park, S. C., Park, M. K., and Kang, M. G. (2003). Super-resolution image reconstruction: A technical overview. *IEEE Signal Processing Magazine*.

Patti, A. and Altunbasak, Y. (2001). Artifact reduction for set theoretic super resolution image reconstruction with edge adaptive constraints and higher-order interpolants. *IEEE Trans. Image Processing*, 10(1):179–186.

Patti, A., Sezan, M., and Tekalp, A. (1997). Superresolution video reconstruction@with arbitrary sampling lattices and nonzero aperture time. *IEEE Trans. Image Processing*, 6(8):1064–1076.

Petrou, M. and Edition, C. P. S. (2011). *Image Processing: the Fundamentals*. WILEY, United Kingdom.

Pratt, W. K. (2001). *Digital Image Processing (3rd Ed): New York*. John Wiley and Sons.

Protter, M., Elad, M., Takeda, H., and Milanfar, P. (2009). Generalizing the nonlocal-means to super-resolution reconstruction. *IEEE Transactions on Image Processing*.

Richardson, W. H. (1972a). Bayesian-based iterative method of image restoration. *Journal of the Optical Society of America*, 62(1).

Richardson, W. H. (1972b). Bayesian-based iterative method of image restoration. *Journal of The Optical Society of America*, 62(1):55–59.

Sanchez-Beato, A. and Pajares, G. (2008). Noniterative interpolation-based super-resolution minimizing aliasing in the reconstructed image. *IEEE Transactions on Image Processing*, 17(10):1817–1826.

Schreiber, W. F. (1970). Wirephoto quality improvement by unsharp masking. *J. Pattern Recognition, 2:111-121*.

Shah, K., Pandya, J., and Vahora, S. (2013). A survey on super resolution image reconstruction techniques. *International Journal of Engineering Research & Technology (IJERT)*, 2(4):1897–1901.

Sroubek, F., Cristobal, G., and Flusser, J. (2007). A unified approach to superresolution and multichannel blind deconvolution. *IEEE Transactions on Image Processing*, 16(9):2322–2332.

van Eekeren, A. W. M., Schutte, K., and van Vliet, L. J. (2010). Multiframe super-resolution reconstruction of small moving objects. *IEEE Transactions on Image Processing*.

Yin, Y., Ruan, Q., and Zhang, T. (2016). An improved super-resolution image reconstruction algorithm. *International Journal of Signal Processing, Image Processing and Pattern Recognition*, 9(3):103–112.

Youmin, G., Xing, Z., Yanning, G., and Zhen, D. (2016). An experimental comparison of super-resolution reconstruction for image sequences. *Proceedings of the 35th Chinese Control Conference*.